

# NO<sub>x</sub> REDUCTION IN BIOMASS GRATE FURNACES BY PRIMARY MEASURES - EVALUATION BY MEANS OF LAB-SCALE EXPERIMENTS AND CHEMICAL KINETIC SIMULATION COMPARED WITH EXPERIMENTAL RESULTS AND CFD CALCULATIONS OF PILOT-SCALE PLANTS

**Alexander Weissinger<sup>1</sup>, Ingwald Obernberger<sup>1,2</sup>, Robert Scharler<sup>1</sup>**  
<sup>1</sup>Institute of Chemical Engineering Fundamentals and Plant Engineering,  
Graz University of Technology, Austria  
Email: [weissinger@glvt.tu-graz.ac.at](mailto:weissinger@glvt.tu-graz.ac.at)  
<sup>2</sup>BIOS – Bioenergy Systems, Sandgasse 47, A-8010 Graz, Austria

## ABSTRACT

Reliable boundary conditions concerning the inlet concentrations of NO<sub>x</sub> precursors (HCN, NH<sub>3</sub>, NO, NO<sub>2</sub>, N<sub>2</sub>O) are necessary for modelling the optimisation of NO<sub>x</sub> reduction in biomass furnaces by primary measures. In the context of the work presented, a method for reducing NO<sub>x</sub> emissions by primary measures is evaluated by combining test runs for fibreboard residues as a nitrogen rich biomass fuel in a lab-scale reactor with the simulation of chemical kinetics of NO<sub>x</sub> formation in the gas phase. Moreover, the simulation results and effects discovered at the laboratory test facility are discussed in comparison with experimental results from a pilot-scale furnace (horizontally moving grate) with a nominal boiler capacity of 440 kW<sub>th</sub> and CFD simulations (Computational Fluid Dynamics) of gas phase combustion performed for this pilot scale plant.

The experimental results for the fibreboard fuel investigated showed NH<sub>3</sub> to be the main species released from the fixed bed. NO is of minor importance, HCN is almost negligible. A maximum release of TFN (total fixed nitrogen) can be detected by an inlet superficial velocity (air flow at inlet/cross section area of the fixed bed at inlet) of 0.06 m/s. The subsequent kinetic simulations used the release behaviour of gaseous compounds from the fuel, which had been investigated within various test runs, as boundary conditions and applied the ideal reaction models plug flow (PFR) and perfectly stirred reactor (PSR) of the software code CHEMKIN 3.5<sup>®</sup>. By means of these simulations, the optimum combustion conditions for NO<sub>x</sub> reduction by primary measures were investigated. Simulations of the reaction kinetics based on the measurement results of the lab-scale experiments showed a strong influence of the oxygen concentration in the reacting gas phase on the TFN and NO<sub>x</sub> reduction potential, and, for the PSR model, also an influence of temperature. Both mechanisms predicted the same trends for these parameters but with diverging TFN reduction rates.

A comparison with results from test runs at the pilot scale furnace and with CFD simulations validated the influence of temperature and oxygen concentration on NO<sub>x</sub> reduction. The presented approach proved to be sufficient for the definition of operating conditions for Low-NO<sub>x</sub> combustion in biomass grate furnaces. However, the a priori prediction of NO<sub>x</sub> emissions as well as additional reduction potential by optimisation measures has not been possible so far. This is due to a strong sensitivity of the predicted NO<sub>x</sub> reduction rates to the reaction mechanism applied as well as to reaction conditions, inlet concentrations of N species and CH<sub>4</sub>. These tasks must be investigated in more detail in future in order to further improve the accuracy of NO<sub>x</sub> prediction.

*Key Words:* biomass combustion, NO<sub>x</sub> reduction, primary measures, reaction kinetics, grate furnaces, fibreboard waste

### Abbreviations

CLD	chemiluminescence detection	SV	superficial velocity
FT-IR	Fourier transform infrared	u	velocity [m/s]
HCN	hydrogen cyanide	x	mass fraction [kg/kg]
NH <sub>3</sub>	ammonia	<u>Indices</u>	
NO	nitrogen oxide	Bed	with respect to the fuel bed
NO <sub>x</sub>	Σnitrogen oxides	Fuel	with respect to the fuel
PFR	plug flow reactor	Inlet	with respect to the inlet conditions
PSR	perfectly stirred reactor	Outlet	with respect to the outlet conditions
r	molar release rate	RF	reaction front
TFN	total fixed nitrogen, Σ(NO <sub>x</sub> , NH <sub>3</sub> , HCN) [mole/mole]	d.b.	dry base
TFC	total fixed carbon, Σ(CO, CO <sub>2</sub> , CH <sub>4</sub> ) [mole/mole]	w.b.	wet base
SR	stoichiometric ratio		

## **INTRODUCTION**

Numerous fixed bed biomass furnaces in the small and medium size range (0.5 to 5 MW<sub>th</sub> nominal boiler capacity) are in operation in Austria. The reduction of NO<sub>x</sub> emissions, in addition to particulate emissions of such plants are a major goal of ongoing research activities. The purpose of the project described in this paper is to reduce NO<sub>x</sub> emissions by primary measures in an economically affordable and efficient way, in order to avoid cost-intensive secondary measures (e.g. Selective Non Catalytic Reduction).

Reliable boundary conditions concerning the inlet concentrations of NO<sub>x</sub> precursors (HCN, NH<sub>3</sub>, NO, NO<sub>2</sub>, N<sub>2</sub>O) are necessary for the optimisation of NO<sub>x</sub> reduction in biomass grate furnaces by theoretical investigations. In this work a method of optimising NO<sub>x</sub> emissions is evaluated by combining experimental test runs for fibreboard as a nitrogen rich fuel on a laboratory test facility with the simulation of chemical kinetics of NO<sub>x</sub> formation in the gas phase. Similar approaches with test facilities investigating a downwards propagating reaction front have been applied for wood chips and for straw [6, 7, 8].

The results of the kinetic simulations are compared with results from experiments on a 440 kW<sub>th</sub> horizontally moving grate furnace and CFD calculations performed for this pilot plant.

## **METHODOLOGY**

The release behaviour of the NO<sub>x</sub> precursors (HCN, NH<sub>3</sub>, NO) from a fixed fuel bed depending on combustion specific parameters was investigated by performing test runs on a laboratory reactor. The flow through the fuel bed was varied in the range of a superficial velocity at inlet SV<sub>inlet</sub> (normalised flow rate per cross section area) from 0.05 m/s to 0.08 m/s for air and with a superficial velocity of 0.08 m/s for varied oxygen concentrations at inlet ranging from 13 vol.% to 21 vol.%. The lab-scale experiments were performed using a newly developed in-situ hot-gas application of FT-IR absorption spectroscopy to measure the release of the relevant gaseous species (CO, CO<sub>2</sub>, CH<sub>4</sub>, NH<sub>3</sub>, H<sub>2</sub>O) from the fuel bed. Additional extractive measurements were performed for the concentrations of NO (chemiluminescence detection), NH<sub>3</sub> and HCN (wet chemical analysis). The time dependent behaviour of nitrogen was also examined with the aim of investigating N kinetics combined with CFD simulation. The time dependent parameters investigated are the SV<sub>outlet</sub> and the normalised mass degradation.

The laboratory scale reactor, shown schematically in Figure 1, is a discontinuously operated pot furnace. The laboratory scale reactor consists of a cylindrical retort (height 35 cm, inner diameter 12 cm), which is heated electrically by two separated PID controlled heating circuits. The fuel was put into a cylindrical holder of 100 mm height and 95 mm in inner diameter. Both parts are made of fibre-reinforced SiC ceramics to avoid reactions of CO, NO and ash with the wall and to avoid oxygen entering the reaction zone. The mounting and vessel for the fuel bed are mounted on a plate, which is placed on a mass balance (Sartorius GP 4001, +/- 0,1 g) and put into the upper part as shown by dotted lines in Figure 1 a.. The combustion air or a O<sub>2</sub>/N<sub>2</sub> mixture is introduced through a porous plate at the bottom of the fuel bed. A liquid sealing filled with a thermo oil (Therminol 66) is used to separate the mass balance and the reactor mechanically. Measurements of the species concentrations in the flue gas directly above the fuel bed are performed with a newly developed hot gas application of in-situ FT-IR absorption spectroscopy (MIDAC M2401, MCT detector with 0.5 cm<sup>-1</sup> resolution). The in-situ FT-IR measurements are performed directly above the fuel bed as shown in Figure 1. A detailed description of the FT-IR in-situ absorption spectroscopy applied is given in [2, 3]. Additionally, NO, HCN, NH<sub>3</sub> are determined using extractive measurement equipment of chemiluminescence detection (CLD) for NO and NO<sub>2</sub> with an ECO Physics 740 ht and wet chemical analysis for HCN and NH<sub>3</sub> using a photometric method for sample analysis (HCN: Method 4500-CN- E. Colorimetric Method 4-39 and NH<sub>3</sub> Method 4500-NH<sub>3</sub> F. Phenate Method 4-108 from "Standard Methods for the Examination of Water and Wastewater", 20<sup>th</sup> edition, 1998 [1]). The flue gas is diluted 1/10 with N<sub>2</sub> (DEKATI DILUTER) before entering the ECO Physics equipment to avoid hazardous conditions. NH<sub>3</sub> and HCN are measured directly without dilution.

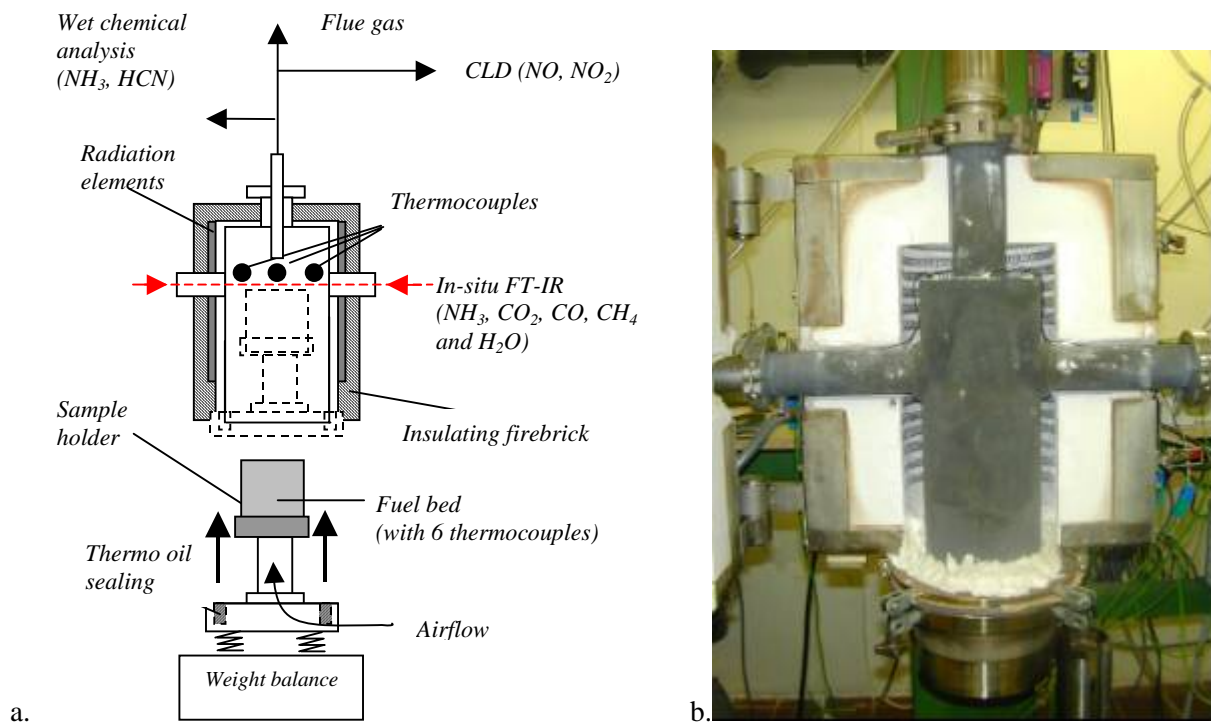


Figure 1. Schematic experimental set-up (a) and picture of the lab-scale pot furnace for the investigation of N release from a fixed bed combined with FT-IR absorption spectroscopy (b).

6 thermocouples are placed in the sample holder of the fuel bed to measure the time dependent temperature distribution in the fuel bed. Five thermocouples are placed within the fuel bed. One thermocouple T Bed 2 is placed in the middle of the diameter, directly beneath

the fuel bed to measure the temperature of the combustion air. A more detailed description of the experimental set-up and discussion of the results of the test runs can be found in [3, 4, 12].

Table 1: Composition (a) and particle size distribution (b) of the fibreboard residues used as fuel for the lab-scale experiments

Fuel type	Moisture	C	H	N	Volatiles	Fixed carbon	Ash	
Fibreboard waste	[wt% w.B.]	[wt%d.B.]						
Test 1	8.60	49.7	5.8	4.0	80.2	17.8	1.9	
Test 2	10.6	50.0	5.8	3.8	80.6	17.7	1.7	
Test 3	11.5	48.0	6.0	3.4	80.0	17.8	2.1	
mean value	10.2	49.2	5.9	3.7	80.5	18.0	1.4	
a standard deviation		0.91	0.11	0.24	0.23	0.07	0.17	

upper limit	lower limit	relative frequency				
[mm]	[mm]	measuring 1	measuring 2	measuring 3	mean value	standard deviation
	> 16,0	0.04	0.03	0.04	0.04	0.01
16.0	10.0	0.28	0.35	0.34	0.32	0.03
10.0	5.0	0.40	0.37	0.36	0.37	0.02
5.0	2.5	0.28	0.26	0.26	0.26	0.01
b	Checksum	1.00	1.00	1.00	1.00	0.00

### *Simulation of reaction kinetics in the gas phase*

The experimental results describing the release of the species measured were used to define the inlet concentrations for chemical kinetic calculations in the gas phase focusing on NO<sub>x</sub> reduction. The NO<sub>x</sub> reaction mechanisms were investigated on the ideal reactor models of a perfectly stirred reactor (PSR) using the AURORA Gas\_PSR program code and a plug flow reactor (PFR) using the SENKIN program code from CHEMKIN 3.5<sup>®</sup>. The optimum conditions for NO<sub>x</sub> reduction by primary measures were investigated by means of parameter studies. Moreover, the stability of the global optimum and the deviations from predicted reduction rates were investigated by means of sensitivity analysis for the main influencing parameters. The calculations were performed for adiabatic models with constant temperature using the GRI 3.0 reaction mechanism [9]. Additional calculations were performed for selected cases using the Kilpinen 97 mechanism [10].

## **EXPERIMENTAL RESULTS FOR THE INFLUENCING PARAMETERS ON N RELEASE AND BOUNDARY CONDITIONS DERIVED FROM THE LAB-SCALE REACTOR TEST RUNS**

The lab-scale test runs showed NH<sub>3</sub> to be the major nitrogen containing species released from the fixed fuel bed for the fuel investigated. NH<sub>3</sub> is mainly released during devolatilisation and in the transition state to charcoal burnout [4, 12]. Afterwards, during charcoal burnout only NO is released, but at a significantly lower level. The release of HCN from the fuel occurred during all test runs at an almost negligible level.

The lab-scale results showed that the velocity of the reaction front propagation  $u_{RF}$  is the only parameter capable of describing the overall NH<sub>3</sub> release during the devolatilisation step (Figure 2 a.) and the transition stage for all test runs.  $u_{RF}$  was calculated for the test runs from the time shift and the distance of the thermocouples at the top and at the bottom of the fuel bed. During charcoal burnout significant amounts of NO are released, but no NH<sub>3</sub>.

The influence of the outlet superficial velocity  $SV_{outlet}$  on the instantaneous  $NH_3$  conversion rates is shown in Figure 2b. These parameters can be described as a time dependent function during the test runs. It can be seen that maximum  $NH_3$  conversion rates occur at a  $SV_{outlet}$  of 0.15 m/s. A more detailed discussion can be found elsewhere [4, 12].

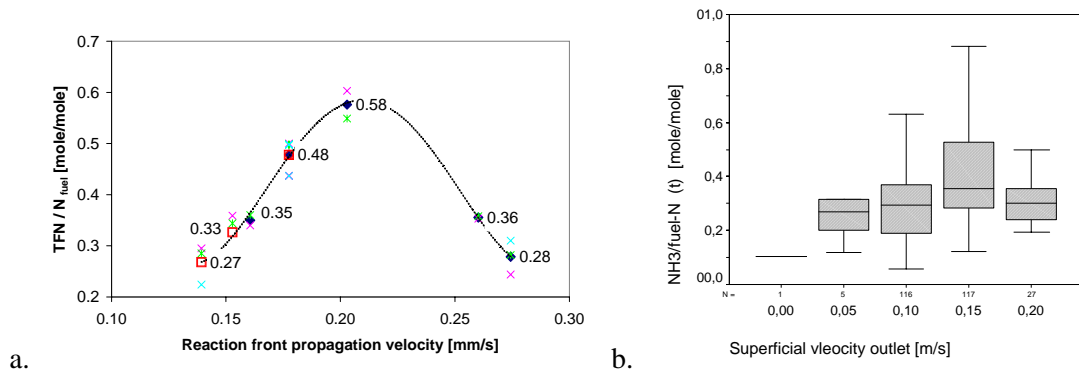


Figure 2: Overall TFN conversion rates during the devolatilisation phase as a function of the reaction front propagation velocity (a) and instantaneous  $NH_3$  conversion rates as a function of the superficial velocity at outlet (b) for the fuel fibreboard  
Explanations: Values are mean values of all test runs for each parameter; ( $\blacklozenge$ )  $SV_{inlet}$  varied between 0.05 m/s and 0.01 m/s,  $O_2$  concentration 21 vol.%; ( $\square$ )  $SV_{inlet}$  0.08 m/s,  $O_2$  concentration varied between 13 - 21 vol.% at laboratory reactor inlet.

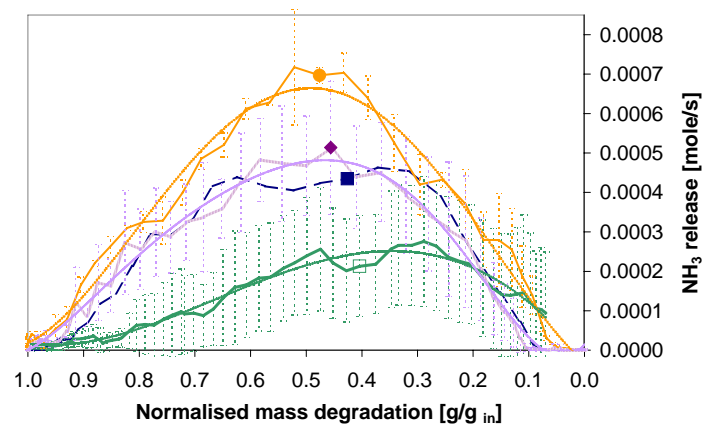


Figure 3:  $NH_3$  release rates as a function of the normalised mass degradation for various reaction front propagation velocities.  
Explanations: The release rate refers to an initial fuel amount of 187 g, a nitrogen content of 4 wt% d.b. and a moisture content of 10 wt% w.b.; the occurring reaction front propagation velocities according to Table 2 are: ( $\circ$ )  $u_{RF}$  0.15 mm/s, ( $\diamond$ )  $u_{RF}$  0.17 mm/s, ( $\square$ )  $u_{RF}$  0.20 mm/s, ( $\blacksquare$ )  $u_{RF}$  0.27 mm/s.

A scaling factor defining the mass flows is necessary for the description of N release from a fuel bed along a grate. A suitable factor for this purpose is the normalised mass degradation as a function of time (Figure 3). It is easier to determine experimentally and theoretically on a grate than a flow rate of product gas, or the  $SV_{outlet}$ . The mass degradation can be determined on a grate by investigating the ash and moisture content of samples taken from different positions at the grate as described in previous papers [13].

From the results presented so far it can be concluded that a two step approach can be applied in a first approximation for theoretical simulation of  $NO_x$  kinetics in the gas phase,

distinguishing between the gasification phase and the charcoal burnout phase. The simulations will be shown in the following chapters.

## RESULTS OF THE CHEMICAL KINETICS SIMULATIONS

### *Boundary conditions applied*

For the theoretical investigations of the NO<sub>x</sub> reaction kinetics a two step approach was chosen for describing N release from the fuel bed. The inlet conditions for the calculations were defined based on the mean concentrations of the gas species occurring during the gasification phase and the charcoal burnout according to the test run conditions, respectively SV<sub>inlet</sub> and reaction front propagation velocity. The gas species concentrations used for the parameter studies are summarized in Table 2.

Table 2: Inlet concentrations and important test run conditions for the kinetic simulations performed.

Explanations: *italic* parameters are varied (O<sub>2</sub> 0.03 to 0.1, N<sub>2</sub> 1-Σy<sub>i</sub>), FT-IR...measured with in-situ absorption spectroscopy; CLD...extractive measurement using chemiluminescence detection (ECO-Physics 1740 ht); SV<sub>inlet</sub>...superficial velocity at inlet; u<sub>RF</sub>...reaction front propagation velocity, calculated from the time shift between thermocouples on top and at the bottom of the fuel bed)

Parameters varied	unit	25 l/min	30 l/min	40 l/min	30 l/min	30 l/min
		21 vol.% O <sub>2</sub>	21 vol.% O <sub>2</sub>	21 vol.% O <sub>2</sub>	16 vol.%O <sub>2</sub>	13 vol.%O <sub>2</sub>
SV <sub>inlet</sub>	m/s	0.06	0.07	0.09	0.07	0.07
u <sub>RF</sub>	mm/s	0.20	0.17	0.27	0.15	0.14
H <sub>2</sub> O_FTIR	[mole/mole]	0.25	0.18	0.20	0.14	0.11
CO <sub>2</sub> _FTIR	[mole/mole]	0.18	0.18	0.17	0.13	0.11
CO_FTIR	[mole/mole]	0.11	0.09	0.10	0.07	0.06
CH <sub>4</sub> _FTIR	[mole/mole]	0.012	0.010	0.011	0.008	0.007
NH <sub>3</sub> _FTIR	[mole/mole]	0.007	0.007	0.005	0.006	0.006
NO_CLD	[mole/mole]	0.0003	0.0002	0.0001	0.0003	0.0004
HCN wet chemical	[mole/mole]	0.000001	0.000002	0.000001	0.000001	0.000000
<b>O<sub>2</sub> (varied)</b>	<b>[mole/mole]</b>	<b>0.03 - 0.1</b>	<b>0.03 - 0.1</b>	<b>0.03 - 0.1</b>	<b>0.03 - 0.1</b>	<b>0.03 - 0.1</b>
<b>N<sub>2</sub> (remainder)</b>	<b>[mole/mole]</b>	<b>0.41 - 0.34</b>	<b>0.50 - 0.43</b>	<b>0.49 - 0.42</b>	<b>0.62 - 0.55</b>	<b>0.67 - 0.60</b>
Total	[mole/mole]	1.00	1.00	1.00	1.00	1.00

The oxygen concentration at inlet was varied from 0.03 mole/mole to 0.1 mole/mole to change the stoichiometry of the gas phase, keeping all other concentrations except N<sub>2</sub> constant. The stoichiometric ratio of the gas phase reactions investigated can be calculated using the following equation:

$$SR_{Gas} = \frac{\frac{x_{O_2}}{x_{fuel\_gas}}}{\left( \frac{x_{O_2}}{x_{fuel\_gas}} \right)_{stoichiometric}} \quad \text{Equation 1}$$

The following restrictions have to be taken into consideration for the calculations: temperatures are defined by experience and varied for the purpose of sensitivity analysis. This was done on the assumption that they can be controlled by flue gas recirculation. The ideal models do not consider the changes in residence time nor changes in the flow field because of higher volume flows at higher temperatures. This is an effect that can only be described by CFD calculations. The calculations presented were performed for mean values of the concentrations measured during the gasification phase as shown in Table 2. Calculations were also performed for the burnout zone with parameters derived from the charcoal burnout in the

lab-scale experiments, but only negligible changes in TFN concentrations occurred in the investigated temperature region [12]. For this reason these calculations are not discussed in this context. The possible influence of mixing with flue gas from the burnout zone was investigated in a sensitivity analysis by varying the inlet concentrations of NO and O<sub>2</sub> inlet.

#### *Effect of inlet concentrations*

Calculations were performed by varying the O<sub>2</sub> concentrations from 0.03 mole/mole to 0.1 mole/mole O<sub>2</sub> in the gas phase. The GRI 3.0 reaction mechanism and the PFR model were used for the kinetic calculations. The calculation results show that the TFN reduction occurs in two steps, a first, very fast NH<sub>3</sub> reaction, supported by radicals producing NO, HCN and N<sub>2</sub>O. In secondary reactions these components partially react to N<sub>2</sub> with a strong influence of residence time (Figure 4).

The comparison of TFN reduction rates is sufficient for the evaluation if the inlet concentrations of TFN stay constant. Regarding the experiments, the influence of changed inlet conditions in particular is investigated and the resulting absolute values of NO<sub>x</sub> emissions are of interest. A comparison of absolute emissions can be made by comparing the TFN/TFC ratio. TFC (Total Fixed Carbon) is a parameter that remains constant during the gas phase combustion (only conversions to CO<sub>2</sub> take place). On this assumption, the ratio allows a direct comparison of absolute concentration values for different inlet conditions, especially concerning the TFN at inlet.

The calculation results show a maximum TFN reduction rate for an inlet oxygen concentration of 0.05 mole/mole for all calculations based on the experiments with air. This results in a mean SR<sub>Gas</sub> range of 0.57 to 0.69, depending on the inlet concentrations. Different inlet concentrations of NH<sub>3</sub> and NO (according to the test runs with varied air flow) showed less influence (Figure 4, Figure 5a). The temperature optimum regarding TFN reduction is located in the region between 950 °C and 1,000 °C (Figure 5a, Figure 5c).

For the lab-scale experiments performed with a gas mixture with reduced oxygen concentrations, a shift of the optimum O<sub>2</sub> inlet concentration and in the temperature dependence was detected. A shift of the optimum O<sub>2</sub> concentration to 0.03 mole/mole was observed (Figure 5b) and for an O<sub>2</sub> concentration of 0.05 mole/mole TFN reduction rates decreased with increasing temperature (Figure 5a). But the achievable optimum TFN reduction rates turned out to be the same for both cases (Figure 5b). In the region of the optimum O<sub>2</sub> concentration the influence of temperature on the TFN emission level is again of minor influence in the temperature region > 1,050 °C (Figure 5d).

A comparison of the influence of the residence time in the primary combustion zone under reducing conditions shows a significant influence of the TFN reduction rates independent of temperature. The calculations for the optimum O<sub>2</sub> concentration of 0.05 mole/mole regarding TFN reduction show an increase of TFN reduction from approximately 87 % after 0.3 s up to 97 % after 0.8 s (Figure 5c).

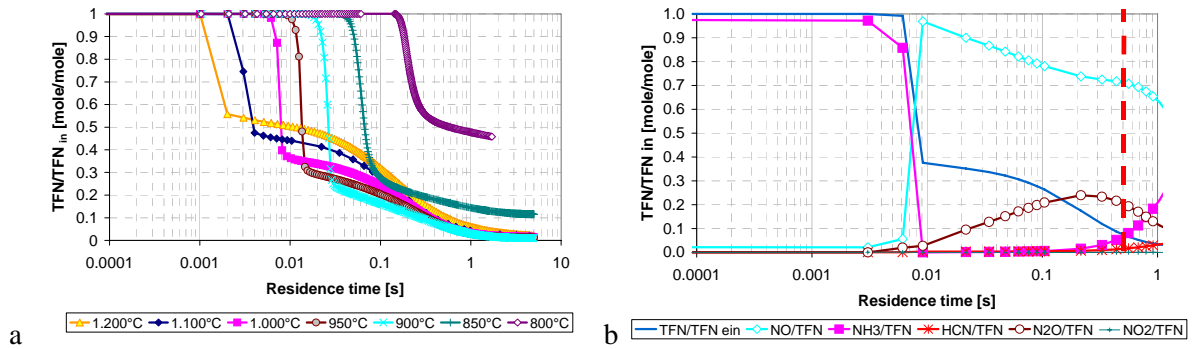


Figure 4: TFN reduction (a) and ratios of major N compounds to TFN (b) as a function of residence time reaction mechanism GRI 3.0  
Explanations: Calculation model: PFR, inlet concentrations according to Table 2; (a) temperature 1,000 °C, O<sub>2</sub> inlet 0.05 mole/mole; (b) temperature 1,000 °C, O<sub>2</sub> inlet 0.05 mole/mole, u<sub>RF</sub> 0.17 mm/s.

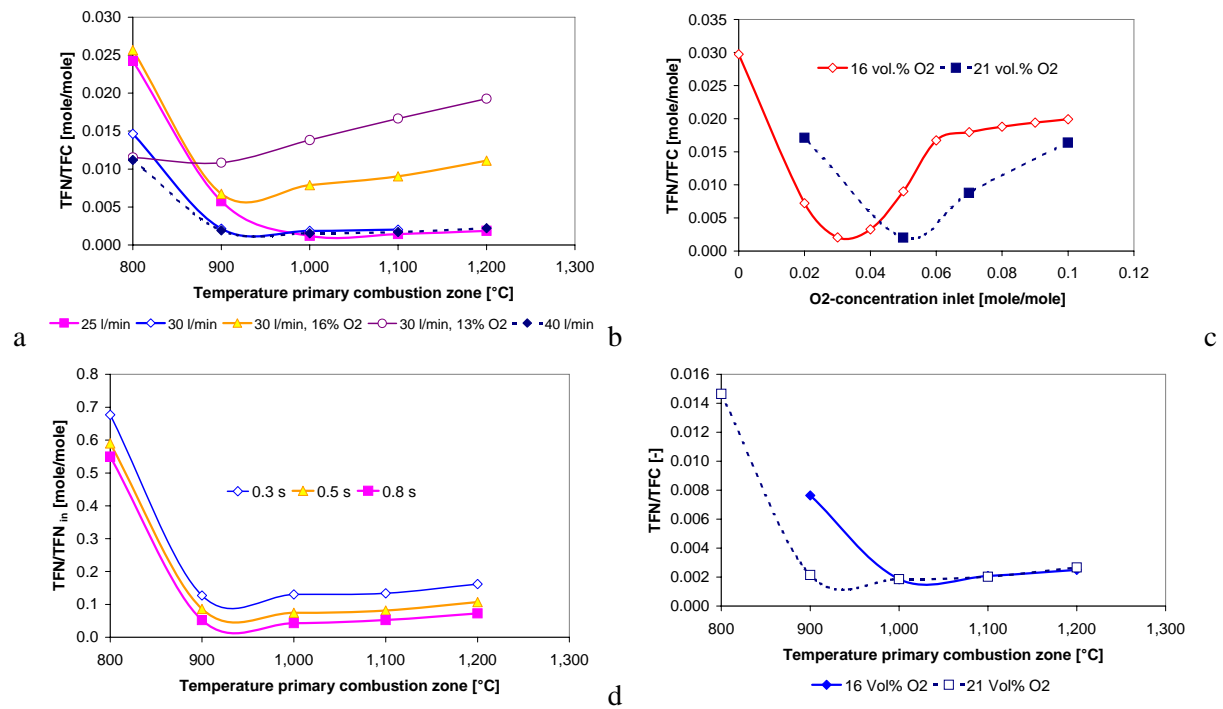


Figure 5: Sensitivity analysis concerning the location of the TFN emission minimum regarding the influence of temperature and oxygen concentration in the gas mixture - reaction mechanism GRI 3.0  
Explanations: Calculation model PFR; residence time in the primary combustion zone 0.5 s; (a) inlet concentrations according to Table 2 with an oxygen concentration of 0.05 mole/mole (b) inlet concentrations according to Table 2, SV<sub>inlet</sub> 0.07 m/s, temperature 1,000 °C, (c) inlet concentrations according to Table 2, SV<sub>inlet</sub> 0.07 m/s (d) inlet concentrations according to Table 2 with an oxygen concentration at its optimum for a TFN minimum (◆) O<sub>2</sub> 0.03 mole/mole, u<sub>RF</sub> 0.15 mm/s and (□) O<sub>2</sub> 0.05 mole/mole u<sub>RF</sub> 0.17 mm/s.

### Sensitivity analysis of TFN inlet composition for the optimum $O_2$ concentration and temperatures

A sensitivity analysis was performed for the conditions derived for maximum TFN reduction rates by changing the inlet concentrations of HCN and NO. The amount of HCN in the inlet gas was raised up to 50% of the original  $NH_3$  amount, keeping the sum of  $NH_3 + HCN$  at its initial value of 7,000 ppm<sub>v</sub> (case  $u_{RF}$  0.17, Table 2). The results show, that higher amounts of HCN lead to higher TFN concentrations at reactor outlet. It must be expected that they finally result in higher  $NO_x$  emissions (Figure 6a). For the calculations of the influence of NO inlet concentrations, the original NO concentration was raised from 165 ppm<sub>v</sub> to 800 ppm<sub>v</sub> keeping all other concentrations constant. As can be seen in Figure 6b, these NO concentrations result in only slight changes in the TFN emission level after a residence time of 0.5 s in the primary combustion zone.

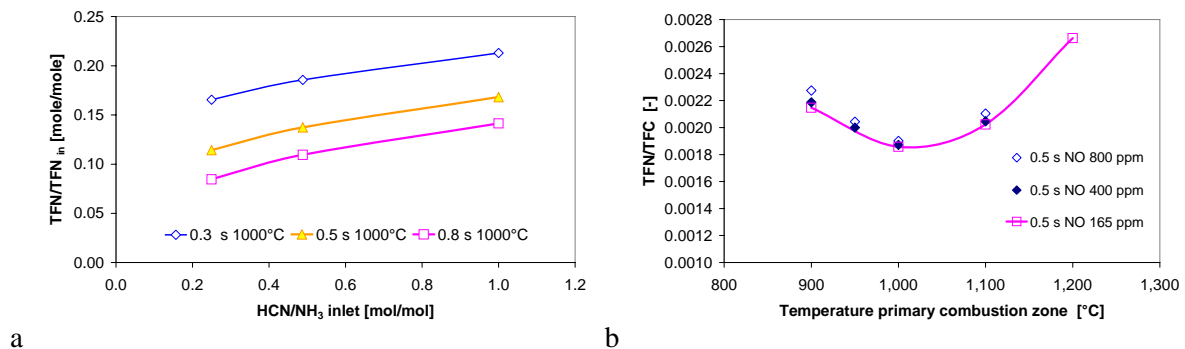


Figure 6: (a) TFN reduction as a function of the HCN/ $NH_3$  ratio in the inlet gas stream after various residence times; (b) influence of temperature on the TFN/TFC ratio for different NO concentrations in the inlet gas  
Explanations: inlet concentrations according to Table 2, (a)  $SV_{inlet}$  0.08 m/s, 21 vol.%  $O_2$ , the sum of HCN +  $NH_3$  was kept constant at 7,000 ppm<sub>v</sub>.(b)  $SV_{inlet}$  0.08 m/s, 21 vol.%  $O_2$ , NO was added to the original concentrations.

### Sensitivity analysis of $H_2$ and $CH_4$ inlet concentrations

$H_2$  could not be measured in the experimental set-up. Hence a sensitivity analysis for the inlet  $H_2$  concentration was performed in order to investigate possible influences. The inlet concentration of  $H_2$  was varied up to twice the concentration of  $CH_4$ . For temperatures over 900 °C higher inlet concentrations of  $H_2$  result in slightly higher TFN reduction rates of approximately 3 to 5%, but the temperature of 1,000 °C for a maximum TFN reduction (Figure 7a) remains constant.

The calculations performed for the sensitivity analysis concerning the inlet concentration of  $CH_4$  showed that this parameter significantly influences the combustion time and the optimum conditions for TFN reduction. Depending on the inlet oxygen concentration, different influence trends of the temperature can be observed. Higher  $CH_4/O_2$  ratios at inlet (achieved by raising the  $CH_4$  concentrations and decreasing the  $CO_2$  concentrations) show a shift of the TFN reduction optimum to higher temperature values. Yet all changes in  $CH_4$  concentration result in lower TFN reduction rates, so the global optimum remains constant (Figure 7 b).

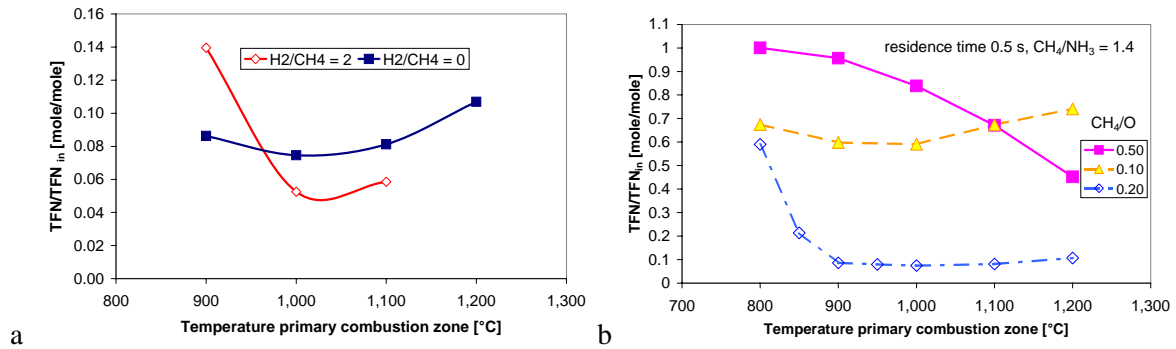


Figure 7: (a) Influence of temperature on TFN reduction for various H<sub>2</sub>/CH<sub>4</sub> ratios in the inlet gas of the primary combustion zone; (b) TFN reduction rates as a function of temperature, for various CH<sub>4</sub>/O<sub>2</sub> ratios at inlet

Explanations: Calculation model PFR; residence time 0.5 s; (a) inlet concentrations H<sub>2</sub>/CH<sub>4</sub>=0: according to Table 2, O<sub>2</sub> concentration of 0.05 mole/mole u<sub>RF</sub> 0.17 mm/s, H<sub>2</sub>/CH<sub>4</sub>=2: H<sub>2</sub> 0.021, H<sub>2</sub>O 0.168, (b) inlet concentrations according to Table 2, u<sub>RF</sub> 0.17mm/s.

### Sensitivity of the reactor model

A sensitivity analysis regarding the global optimum of TFN reduction derived by calculations using the PFR model and the GRI 3.0 mechanism was performed for the PSR model to investigate the influence of the reactor model on the NO<sub>x</sub> reduction trends, the TFN reduction rates and the stability of the derived global optimum concerning different flow conditions. The calculations show a changing trend of the temperature influence on TFN reduction. Contrary to the PFR model, increasing TFN reduction rates can be achieved with increasing temperatures. Nevertheless, the maximum achievable TFN reduction rates of the PFR model are higher than those of the PSR model (Figure 4, Figure 8).

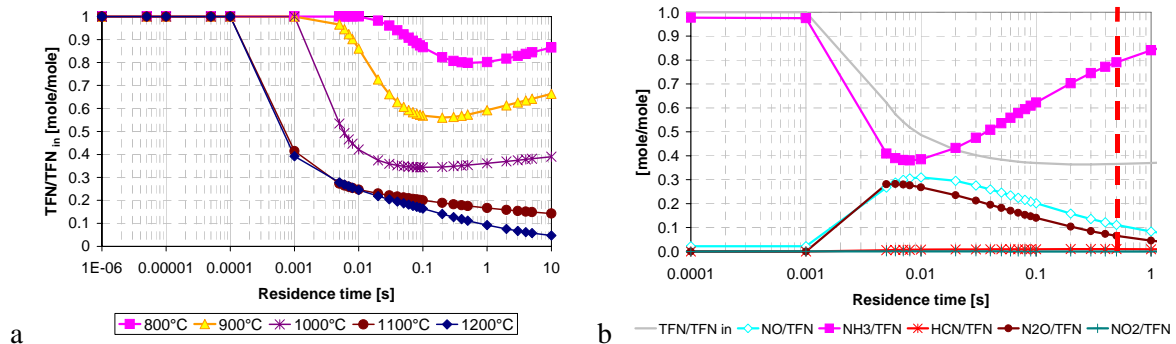


Figure 8: TFN reduction (a) and ratios of major N compounds to TFN as a function of reaction time (b) calculated with the PSR model using the GRI 3.0 mechanism

Explanations: Inlet concentrations according to Table 2 u<sub>RF</sub> 0.17 mm/s with O<sub>2</sub> in the inlet gas of 0.05 mole/mole (b) temperature 1,000 °C.

As Figure 8b shows in comparison to Figure 4b, which was calculated based on the same inlet conditions, there is a certain difference in the composition of the TFN after the primary combustion zone of the PSR model compared to the PFR model. Under strong mixing conditions (PSR), NH<sub>3</sub> is rebuilt after a residence time of 0.1 s for temperatures below 1,000 °C and the TFN rises with increasing residence time. After 0.5 s a TFN reduction rate of 63 % is achieved, but the remaining TFN still consists of 80 % NH<sub>3</sub> compared to a reduction rate of approximately 92 % and a NH<sub>3</sub>/TFN ratio of less than 10 % achieved by

applying the PFR model. Hence, in case of the PSR model the combustion conditions after secondary air addition become an important influence on  $\text{NO}_x$  reduction. Higher reduction potentials in the secondary combustion chamber are more likely to result from higher  $\text{NH}_3/\text{TFN}$  ratios than for higher  $\text{NO}/\text{TFN}$  ratios according to the fast  $\text{NH}_3$  oxidation step.

### Sensitivity of reaction mechanisms

To obtain information on whether the derived optimum conditions remain constant and to quantify the deviation of predicted  $\text{NO}_x$  emissions, the effects of different reaction mechanisms have been tested for the primary and the secondary combustion chamber by applying the Kilpinen 97 reaction mechanism [9]. The GRI 3.0 mechanism predicts a TFN reduction in two steps for the PFR model (Figure 9a). The first reaction step produces higher TFN reduction rates with increasing temperature, resulting also in a faster reaction. During the secondary reaction step TFN reduction is increased by decreasing temperature with a strong influence of residence time. The Kilpinen 97 reaction mechanism shows no secondary TFN reduction reaction via a  $\text{N}_2\text{O}$  path as predicted by the GRI 3.0. The optimum temperature for maximum TFN reduction is 50 °C lower (Figure 9a). The oxygen concentration at inlet for maximum TFN reduction has the same value of 0.05 mole/mole as for GRI 3.0. The differences between the predictions of the two mechanisms can be seen by comparing Figure 9b with Figure 4b.

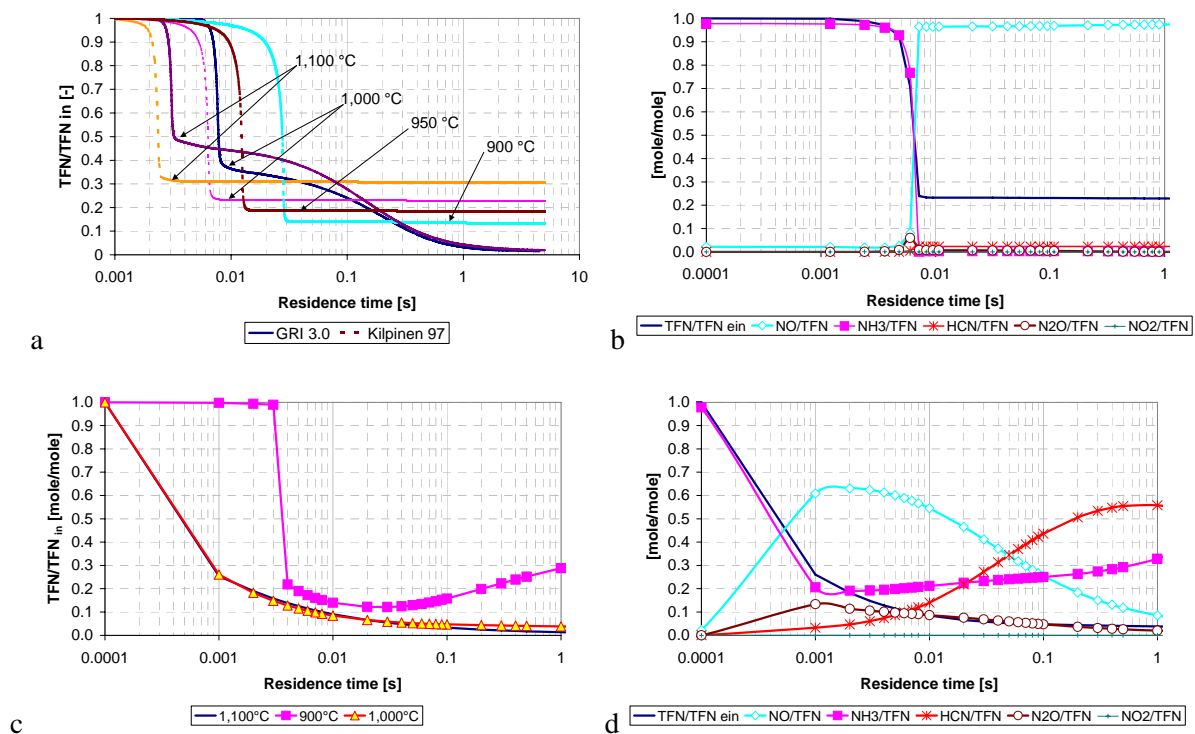


Figure 9 TFN/TFN<sub>in</sub> ratios as a function of residence time at different temperatures, compared for the GRI 3.0 and Kilpinen 97 mechanisms (a, b) and ratios of major N components to TFN as a function of residence time using the Kilpinen 97 reaction mechanism (b, d)  
Explanations: calculation model PFR (a) and (b), PSR (c) and (d); inlet concentrations for all calculations according to Table 2,  $u_{\text{RF}}$  0.17 mm/s,  $\text{O}_2$  0.05 mole/mole; (b), (d) temperature 1,000 °C.

The Kilpinen 97 mechanism predicts higher amounts of HCN produced (HCN/TFN up to 5%), but therefore more than 90% of TFN is converted to NO during NH<sub>3</sub> oxidation (Figure 9b). For this reason lower TFN reduction rates are achieved and no influence of the residence time is predicted and no additional reduction effect in a secondary combustion zone can be expected. For the PSR model the same trends concerning the location of the optimum temperature region and O<sub>2</sub> concentration in the reacting gas-phase predicted by the GRI 3.0 mechanism are validated by the Kilpinen 97 mechanism (Figure 9). Yet for the Kilpinen 97 mechanism the predicted TFN conversion rates for the PSR model are significantly lower than for the PFR model.

### Secondary combustion chamber

Parametric studies for the investigation of the optimum conditions and for TFN reduction rates in the secondary combustion zone were performed by simulations assuming a primary combustion zone with a temperature of 950 °C and a residence time of 0.5 s referring to the optimum conditions regarding TFN reduction in a primary combustion zone calculated as PFR. The inlet concentrations for the secondary combustion zone are given in Table 3.

As general trend could be observed that for the secondary combustion zone a better TFN reduction can be achieved with increasing temperatures. For temperatures above 1,000 °C an influence of O<sub>2</sub> concentration in the gas could no longer be detected (Figure 10a).

Table 3: Inlet concentrations for the parametric studies of the secondary combustion chamber  
Explanations: calculation model PFR, inlet concentrations according to Table 2,  $u_{RF}$  0.17 mm/s, O<sub>2</sub> concentration 0.05 mole/mole temperature 950 °C, residence time in the primary combustion zone 0.5 s; O<sub>2</sub> was varied from, 0.05 to 0.15 mole/mole for the calculations of the secondary zone.

Species	H2	H	O2	OH	H2O	CH4	CO	CO2
HCN/NH3 = 0 [mol/mol]	0.01417	2.7E-06	0.04762	3.2E-07	0.19183	8.8E-08	0.02939	0.24435
HCN/NH3 = 1 [mol/mol]	0.01403	3.1E-06	0.04762	4.7E-07	0.18832	1.1E-09	0.03120	0.24548

Species	NH3	NO	N2O	HNO	HCN	HNCO	N2
HCN/NH3 = 0 [mol/mol]	0.00003	0.00031	0.00010	3.3E-08	0.00001	6.0E-07	0.47220
HCN/NH3 = 1 [mol/mol]	0.00006	0.00032	0.00004	3.1E-08	0.00067	2.4E-06	0.47224

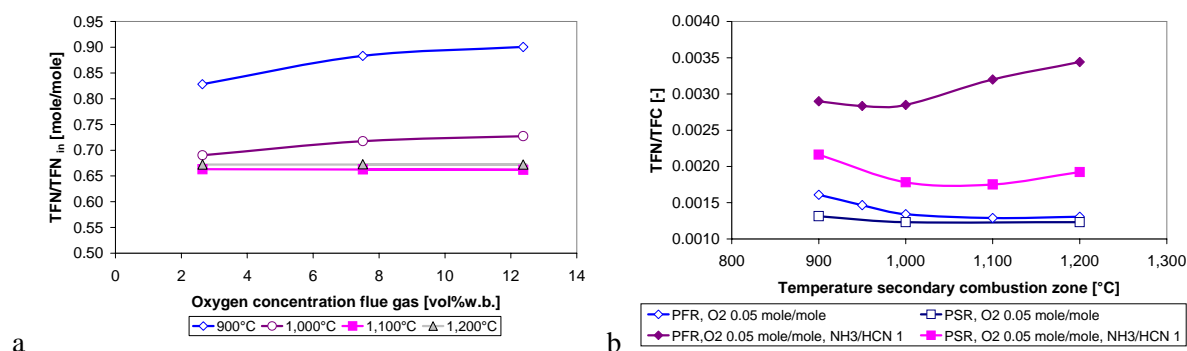


Figure 10: TFN reduction in the secondary combustion zone as a function of the oxygen concentration (a) and for different reactor models as a function of time for various HCN inlet concentrations(b)

Explanations: inlet concentrations according to Table 3, residence time in the primary combustion zone 0.5 s, temperature 950 °C; residence time in the secondary combustion chamber 0.4 s, O<sub>2</sub>-fraction after mixing with secondary air 0.05 mole/mole.

A sensitivity analysis was also performed for the investigation of the influence of the temperature in the secondary combustion chamber for higher HCN inlet concentrations. The calculations were performed with the GRI 3.0 mechanism. As can be seen in Figure 10b, the PSR model predicts the lowest TFN emission levels independent of HCN inlet concentration and temperature. For high amounts of HCN at inlet an increase of the TFN/TFC ratio can be detected with increasing temperatures.

### Modelling a staged combustion

In addition, calculations were performed for a cascade of two PSR models and of two PFR models to simulate a staged combustion. As can be seen in Figure 11, the predicted TFN emission levels, which after the secondary combustion zone refer to NO<sub>x</sub> emission levels, differ strongly for the reactor models and reaction mechanisms applied, although the same tendencies concerning temperature influence and O<sub>2</sub> concentration are predicted by both mechanisms (see former chapter). The strongest variation can be seen by applying the PSR model. This model shows a strong influence of the secondary combustion zone on TFN reduction, which can be explained by higher predicted NH<sub>3</sub> concentrations after the primary combustion zone. The Kilpinen 97 mechanism predicts an extremely good TFN reduction, which seems to over-predict the TFN reduction rates compared to experimental measurements. On the contrary, the GRI 3.0 mechanism predicts an unrealistically high emission level for the PSR cascade which was never measured at the pilot plant. Similar high emission levels are predicted by the Kilpinen 97 mechanism for the PFR cascade. For plug flow conditions, however, the GRI 3.0 predicts more optimistic values than Kilpinen 97. For the PFR model no significant influence of the secondary combustion zone can be seen.

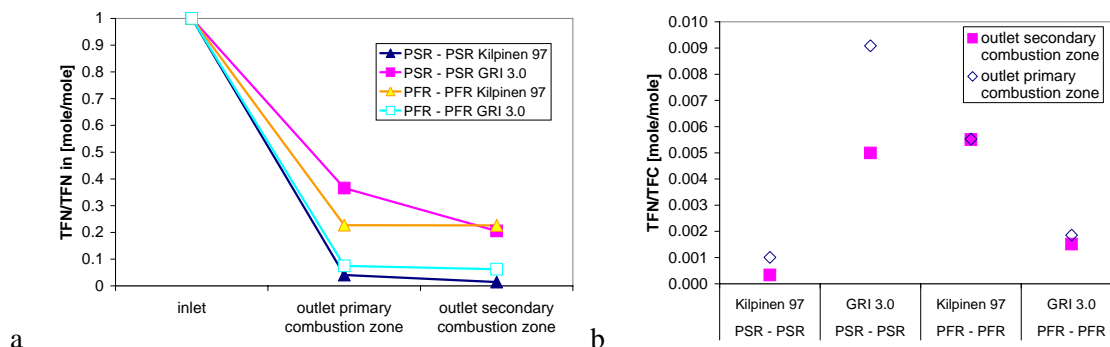


Figure 11: Predicted TFN reduction rates (a) and emission levels (b) after a primary combustion zone and a secondary combustion zone calculated as a cascade of two PSR or two PFR models - comparison of the reaction mechanisms Kilpinen 97 and GRI 3.0

Explanations: Inlet concentrations according to Table 2,  $u_{RF} = 0.17$  mm/s O<sub>2</sub> 0.05 mole/mole, residence time primary combustion zone 0.5 s, temperature 1,000 °C; residence time secondary combustion chamber 0.4 s, O<sub>2</sub> after mixing with secondary air 0.05 mole/mole.

## COMPARISON WITH EXPERIMENTAL RESULTS AND CFD CALCULATIONS

A comparison with experimental results achieved from a pilot plant equipped with a horizontally moving grate furnace showed that the predicted tendencies regarding the influencing parameters discussed are in good agreement with the kinetic calculations for both mechanisms [12]. Due to the flue gas recirculation above the fuel bed the temperature decreased, showing decreasing NO<sub>x</sub> emissions during test runs at the pilot furnace. Oxygen input by flue gas recirculation resulted in reaction conditions comparable to the optimum conditions from the kinetic calculations. An initial O<sub>2</sub> concentration level of about 0.05 to 0.03 mole/mole above the fuel layer was also predicted by CFD calculations of the furnace using the operating data of the plant during the measurements as input (Figure 12a). Taking into consideration these effects discovered at the pilot plant, the PFR model seems to be better applicable. The comparison of actual furnace emissions with the predicted level of the simulations showed a strong variation for both mechanisms. The predicted NO<sub>x</sub> emissions are estimated by the following equation,

$$[NO_x] = [CO_2] \cdot \frac{TFN}{TFC} \cdot \frac{MG_{NO_2}}{22,4} 10^4, \quad [mg/Nm^3] \quad \text{Equation 2}$$

with the concentration [CO<sub>2</sub>] in vol.% in the dry flue gas, MG<sub>NO<sub>2</sub></sub> the molecular weight of NO<sub>2</sub>, and 22.4 the specific mole volume in litre/mole.

Emissions ranging from approximately 160 mg/Nm<sup>3</sup> at an O<sub>2</sub> concentration of 13 vol% d.b. in the flue gas to more than 980 mg/Nm<sup>3</sup> (referring to TFN/TFC ratios between 0.0005 and 0.006) were predicted, compared to a range of 280 mg/Nm<sup>3</sup> to 400 mg/Nm<sup>3</sup> measured at the pilot plant.

A PFR-PFR cascade using the GRI 3.0 showed a realistic value in the order of the measured emissions. For PFR conditions in the primary combustion zone a TFN reduction potential of 20% was predicted for increasing residence times from 0.5 s to 0.8 s. This potential could also be detected during the measurements at the pilot plant. The Kilpinen 97 mechanism in comparison predicted NO<sub>x</sub> emissions 50 % lower for the PSR-PSR cascade, but this seems to be too optimistic and cannot be interpreted as future potential. For the PFR model no dependency of NO<sub>x</sub> reduction of residence time is predicted by the Kilpinen 97 mechanism. If the value of turbulent kinetic energy is taken as a measure for PSR conditions then the regions around the nozzles should be interpreted as PSR, the other part of the furnace seems to behave as PFR (Figure 12b).

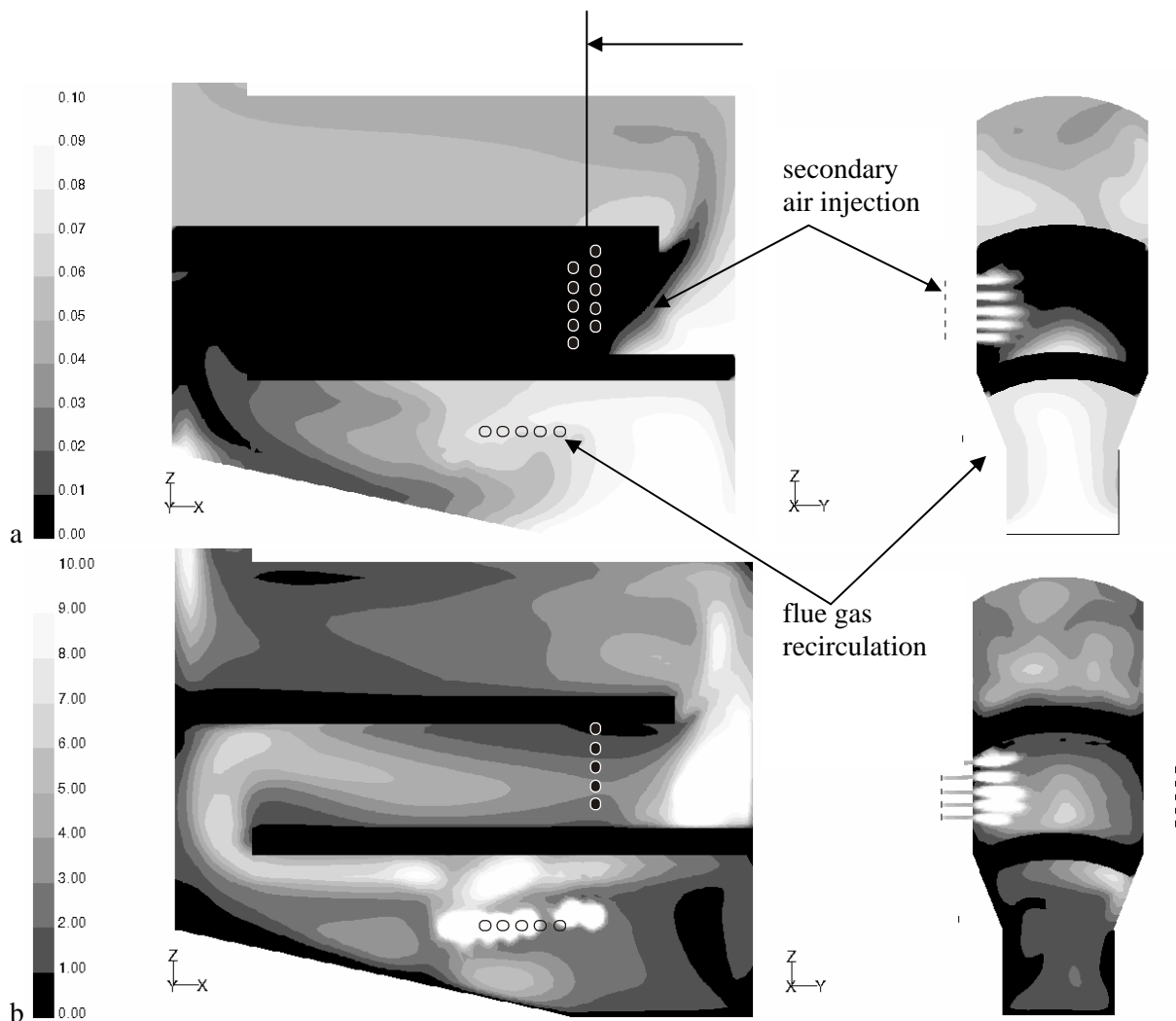


Figure 12:  $O_2$  concentrations (a) and turbulent kinetic energy (b) in the gas phase of the pilot scale furnace calculated with CFD

Explanations: fuel fibreboard, boiler load 430 kW, SR primary combustion zone 0.97, flue gas recirculation above the grate 390 kg/h; the calculations were performed based on operating data for test runs at the pilot-scale plant [12]; (a) units [mole/mole], (b) units [ $m^2/s^2$ ].

## SUMMARY AND CONCLUSIONS

A new method for the optimisation of  $NO_x$  reduction by primary measures for biomass grate furnaces was evaluated. Lab-scale reactor experiments for fixed bed combustion were performed, using a newly developed application of FT-IR in-situ absorption spectroscopy for the determination of species concentrations directly above the fuel bed, in order to investigate their release behaviour. Test runs were performed by varying the gas flow through the fuel bed and varying the  $O_2$  concentration in the gas flow.

The investigations for fibreboard as fuel showed that  $NH_3$  is the major N species released from the fuel bed. HCN only occurred at a negligible level, a thoroughly unexpected result. The overall  $NH_3$  conversion rates of the test runs show a good correlation with the reaction front propagation velocity measured in the fuel bed. NO showed no tendency in dependence

of the parameters varied. The instantaneous  $\text{NH}_3$  release rates can sufficiently be described as functions of the  $SV_{\text{outlet}}$  and the normalised mass degradation rate, which themselves depend on  $\text{O}_2$  concentration at inlet of the fuel layer and gas flow through the fuel bed. Using empirical (fitted) functions the N release profiles for a grate can also be defined and adapted to experimental results, with the advantage that this only requires a description of the mass degradation along a grate and the information of flow conditions along the grate or the  $u_{\text{RF}}$ . For different boundary conditions (gas flow, oxygen concentration, reaction front propagation rate) the  $\text{NH}_3$  release profile can be described as a function of the normalised mass degradation. This approach is especially interesting for the definition of N release profiles for CFD applications, based on kinetic models for pyrolysis and combustion.

A two step approach for the description of the release behaviour was chosen for the definition of the inlet concentrations for studies of chemical reaction kinetics in the gas phase, based on the experimental results.

The results of the studies of  $\text{NO}_x$  reaction kinetics in the gas phase for a primary combustion zone using the PFR model indicated maximum TFN reduction in a temperature region between  $950\text{ }^\circ\text{C}$  and  $1,000\text{ }^\circ\text{C}$  and an initial  $\text{O}_2$  concentration in the reacting gas phase of 0.05 mole/mole. This optimum is predicted by the GRI 3.0 mechanism and the Kilpinen 97 mechanism and remains stable within a range of  $\pm 50\text{ }^\circ\text{C}$  for all variations of inlet concentrations according to the reactor experiments. The PSR model showed the same optimum regarding the oxygen concentration, but a shift to higher reduction rates was observed at higher temperatures for both mechanisms. In the PSR model a significant amount of  $\text{NH}_3$  is formed after a residence time of 0.1 s. This also leaves a higher reduction potential for a secondary combustion zone.

The calculation results of the PFR model for changing inlet concentrations according to the reactor experiments with a reduced oxygen concentration show a shift of the maximum TFN reduction rates to an  $\text{O}_2$  inlet concentration of 0.03 mole/mole and a temperature of  $1,000\text{ }^\circ\text{C}$ . Yet the potential TFN emissions after the primary combustion zone, represented by the TFN/TFC ratio remained constant.

A sensitivity analysis concerning the residence time in the primary combustion zone showed that for PFR conditions a TFN reduction potential of more than 50 % can be achieved by raising the residence time from 0.3 s to 0.8 s and of about 20 % by raising it from 0.5 s to 0.8 s as predicted by the GRI 3.0 mechanism but not the Kilpinen 97 mechanism. This potential could also be detected during the test runs at the pilot scale plant. For the PSR model the TFN amount rises with residence time for temperatures lower than  $1,000\text{ }^\circ\text{C}$  for both mechanisms.

Higher HCN inlet concentrations generally lead to lower reduction rates and higher TFN emissions after the primary combustion zone, which cannot be reduced in a secondary combustion zone either. So HCN generally raises the  $\text{NO}_x$  emissions irrespective of whether it is released from the fuel or formed (predicted) in the primary combustion zone. On the contrary higher NO inlet concentrations do not affect the TFN emission level. Higher NO inlet concentrations are compensated by higher reduction rates.

$\text{H}_2$  was investigated for different inlet concentrations. It showed no strong influence on the TFN reduction rates, but it accelerates the TFN reduction reaction.  $\text{CH}_4$  on the contrary delays this reaction reducing the achievable TFN reduction rates and increasing the  $\text{NH}_3/\text{TFN}$  ratio. Increasing temperature and  $\text{O}_2$  concentration can again accelerate this reaction. The  $\text{CH}_4$  concentration in the gas can therefore influence the optimum  $\text{O}_2$  concentration as well as the optimum temperature for the TFN reduction and should therefore be investigated in more detail.

Calculations were performed for modelling a staged combustion by a cascade of two PFR models and two PSR models comparing the reaction mechanisms GRI 3.0 and Kilpinen 97. The results showed a strong variation in the predicted TFN reduction rates between the models and reaction mechanisms applied. GRI 3.0 in combination with a PFR-PFR cascade showed the best agreement with NO<sub>x</sub> emissions measured at a pilot-scale furnace, but unrealistically high emissions for the PSR-PSR cascade. The Kilpinen 97 mechanism on the contrary seemed to overpredict the NO<sub>x</sub> reduction for the PSR-PSR cascade and is likely to predict excessive emissions for the PFR-PFR cascade. In case of the PSR cascade a large amount of TFN is reduced in the secondary combustion zone, whereas the PFR showed less influence.

A comparison of kinetic simulation results with the test runs at the pilot-scale furnace showed an agreement of the trends predicted. Yet the NO<sub>x</sub> emissions predicted by the kinetic simulations vary strongly concerning the reactor model and reaction mechanism applied. Additional CFD calculations showed that the test runs were performed for operating conditions in the optimum region predicted by kinetic simulations. An improvement of the NO<sub>x</sub> prediction may be achieved by implementing NO<sub>x</sub> kinetics into CFD calculations. For the generation of boundary conditions the N release model based on the normalised mass degradation and reaction front propagation velocities derived from lab-scale experiments should be applied. This would result in a description of NO<sub>x</sub> formation taking the real flow and temperature conditions in the furnace into consideration. But in this case the development of reduced mechanisms or global mechanisms is necessary due to restrictions of calculation capacity. The results of the calculations still may strongly vary with the reaction mechanisms applied. Hence, more investigations have to be done concerning the ranges of applicability for existing NO<sub>x</sub> reaction mechanisms for biomass applications.

In conclusion it may be stated that the presented method proved to be able to evaluate the relative potentials and the optimum operating conditions of furnaces for N-rich fuels. The temperature in the primary combustion zone should be in the range between 950 °C and 1,050 °C and the O<sub>2</sub> concentration in the initial gas mixture above the fuel layer should be 0.05 mole/mole. In the secondary reaction zone temperatures between 1,000 °C and 1,200 °C should be achieved, in this case the O<sub>2</sub> concentrations in the secondary combustion zone only have negligible influence on NO<sub>x</sub> emissions. So far the method presented is not capable of predicting NO<sub>x</sub> emission levels. This is due to its relatively strong sensitivity to the parameters of the reactor model and the reaction mechanism applied, an additional uncertainty is caused by the sensitivity to CH<sub>4</sub> and HCN inlet concentrations. These parameters must be known as accurately as possible. Further investigations are therefore recommended in this context.

## **ACKNOWLEDGEMENT**

This work was supported by the Austrian Industrial Research Promotion Fund (FFF), the Austrian Federal Ministry of Transport, Innovation and Technology and the company MAWERA Wood Combustion Systems in Hard/Austria.

## REFERENCES

1. CLESCERI L. S., GREENBERG A. E., EATON A. D., 1998: Standard Methods for the Examination of Water and Wastewater, 20<sup>th</sup> edition, ISBN 0-87553-235-7, 1998
2. FLECKL T, JÄGER H and OBERNBERGER I. 2000: Combustion diagnostics at a biomass-fired grate furnace using FT-IR absorption spectroscopy for hot gas measurements. Proceedings of the 5th European Conference on Industrial Furnaces and Boilers, April 2000, Porto, Portugal, ISBN-972-8034-04-0, INFUB (ed), Rio Tinto, Portugal
3. FLECKL T, OBERNBERGER I and WEISSINGER A. 2001: Application of FT-IR in-situ absorption spectroscopy for the investigation of the release of gaseous compounds from biomass fuels in a laboratory scale reactor. Part I: Modification of the FT-IR in-situ absorption spectroscopy, submitted for publication, December 2001.
4. FLECKL T, OBERNBERGER I and WEISSINGER A. 2001: Application of FT-IR in-situ absorption spectroscopy for the investigation of the release of gaseous compounds from biomass fuels in a laboratory scale reactor. Part II: Evaluation of the N-release as function of combustion specific parameters, submitted for publication December 2001.
5. GORT R 1995: On the propagation of a reaction front in a packed bed thermal conversion of municipal solid waste and biomass, PhD thesis University of Twente, ISBN 90-9008751-6, Netherlands.
6. LECKNER B and THUNMAN H. 2000: Ignition and propagation of a reaction front in cross-current bed combustion of wet biofuels, FUEL vol. 80 (2001) pp.473-481, Elsevier Science Ltd. (Ed.), Oxford, UK.
7. SAASTAMOINEN J.J., TAIPALE R, HORTTANAINEN M and SARKOMA P. 2000: Propagation of the Reaction front in Beds of Wood Particles, COMBUSTION AND FLAME Vol. 123: pp.214 –226, Elsevier Science Inc.
8. VAN DER LANS R.P., PEDERSEN, L.T., JENSEN A., GLARBORG P. and DAM-JOHANSEN K. 1999: Straw combustion in grate furnaces. In: Addendum Proceedings of the 4th Biomass Conference of the Americas, Sept 1999, Oakland (California), USA, ISBN 0 08 043019 8, Elsevier Science Ltd. (Ed.), Oxford, UK.
9. SMITH G.P., GOLDEN D.M., FRENKLACH M., MORIARTY N.W., EITENEER B., GOLDENBERG M., BOWMAN C.T., HANSON R.K., SONG S., GARDINER W.C. Jr., LISSIANSKI V.V. and QIN Z. 2000: [http://www.me.berkeley.edu/gri\\_mech/](http://www.me.berkeley.edu/gri_mech/)
10. KILPINEN, P., Åbo Akademi University - PCG, Detailed Kinetic Scheme "Kilpinen 97", 1997: <http://www.abo.fi/fak/ktf/cmc>.
11. KELLER R. 1994: Primärmaßnahmen zur NO<sub>x</sub> Minderung bei der Holverbrennung mit dem Schwerpunkt Luftstufung, Forschungsbericht Nr. 18 (1994), Laboratorium für Energiesysteme ( Hrsg.), ETH Zürich, Schweiz.
12. WEISSINGER A. 2002: Experimentelle Untersuchungen und theoretische Simulationen zur NO<sub>x</sub>-Reduktion durch Primärmaßnahmen bei Rostfeuerungen, PhD-thesis, Graz University of Technology, Austria
13. WEISSINGER A. 1999: NO<sub>x</sub> reduction by primary measures on a traveling-grate furnace for biomass and waste wood. In: Proceedings of the 4<sup>th</sup> Biomass Conference of the Americas, Sept 1999, Oakland (California), USA, ISBN 0 08 043019 8, Elsevier Science Ltd. (Ed.), Oxford, UK, pp. 1417-1425.